applied sciences

MDPI

Article

Sensitive Ant Algorithm for Edge Detection in Medical Images

Cristina Ticala *,†, Camelia-M. Pintea † and Oliviu Matei †

Technical University of Cluj-Napoca, North University Center of Baia Mare, 400114 Cluj-Napoca, Romania; dr.camelia.pintea@ieee.org (C.-M.P.); oliviu.matei@holisun.com (O.M.)
* Correspondence: cristina.ticala@cunbm.utcluj.ro
† These authors contributed equally to this work.

Abstract: Nowadays, reliable medical diagnostics from computed tomography (CT) and X-rays can be obtained by using a large number of image edge detection methods. One technique with a high potential to improve the edge detection of images is ant colony optimization (ACO). In order to increase both the quality and the stability of image edge detection, a vector called pheromone sensitivity level, PSL, was used within ACO. Each ant in the algorithm has one assigned element from PSL, representing the ant's sensibility to the artificial pheromone. A matrix of artificial pheromone with the edge information of the image is built during the process. Demi-contractions in terms of the mathematical admissible perturbation are also used in order to obtain feasible results. In order to enhance the edge results, post-processing with the DeNoise convolutional neural network (DnCNN) was performed. When compared with Canny edge detection and similar techniques, the sensitive ACO model was found to obtain overall better results for the tested medical images; it outperformed the Canny edge detector by 37.76%.

Keywords: medical image edge detection; image processing; fixed point; Krasnoselskij iteration; admissible perturbation; ant colony optimization

Citation: Ticala, C.; Pintea, C.-M.; Matei, O. Sensitive Ant Algorithm for Edge Detection in Medical Images. *Appl. Sci.* **2021**, *11*, 11303. https://doi.org/10.3390/app112311303

Academic Editor: Peng-Yeng Yin, Ray-I Chang, Youcef Gheraibia, Ming-Chin Chuang, Hua-Yi Lin and Jen-Chun Lee

Received: 1 November 2021
Accepted: 22 November 2021
Published: 29 November 2021

1. Introduction

Today, medicine is interconnected with technology. Human injuries caused by accidents or other similar events can be detected and correctly diagnosed by using tomography or X-rays. In medical image processing, edge detection has a major role. In order to obtain accurate medical diagnoses, the best computing models are involved. As swarm intelligence has a huge impact nowadays in solving complex problems, the current work uses a particular swarm method, ant colony optimization (ACO) [1], to solve the edge detection problem.

Learning is one of the most efficient artificial intelligence capabilities; in [2], learning with PDE-based CNNs and dense nets for the purpose of detecting COVID-19, pneumonia, and tuberculosis from chest X-ray images was studied. In the same context, automatic COVID-19 detection from chest X-ray and CT-scan images was proposed [3] within a new meta-heuristic feature selection using an optimized convolutional neural network [4].

"A meta-heuristic is an iterative master process that guides and modifies the operations of subordinate heuristics to efficiently produce high-quality solutions" [5]. In general, the quality of heuristics solutions, including bio-inspired methods such as ACO, is given by appropriate probabilistic assumptions [6].

One of the most recent works related to medical image edge detection with ant colony optimization shows the efficiency of a gradient-based ant spread modification to ACO for retinal blood vessel edge detection [7]. In [8], a new image filtering method is introduced for the problem of edge extraction for some targets according to the top-down information based on the image perspective effect; the authors assign scale and orientation, in a hard manner, in order to enhance a local edge detection.

Ant colony optimization is one of the most successful metaheuristics used within complex combinatorial optimization problems, as, for example, in scheduling, transportation and test case prioritization problems [9–12]. Pintea and Pop introduced and showed the benefits of agent sensitivity, including sensitive robots, in security-related problems [13,14], such as a denial jamming attack on sensor networks. As a reference, the current work makes use of the state-of-the-art Canny [15] edge detection technique. Recently, the Canny operator was used in [16] during a symmetrical difference kernel SAR image edge detection process.

The current paper introduces a version of ant colony method with a specific feature called pheromone sensitivity level, PSL, for solving the medical edge detection problem. The artificial ants are endowed with different levels of artificial pheromone sensitivity; thus, the agents have different reactions in a dynamic environment. Here, the new algorithm is applied to the image edge problem and requires a heuristic value computed with two admissible perturbation operators applied to a demicontractive mapping.

Pintea and Ticala proposed the first related theoretical approach in [17]; a step forward was made in [18]. It includes more tests for both ant colony versions of medical image edge detection and a comparison of these techniques; details, including the efficiency of the new parameters and the use of some demicontractive operators, are presented.

The current work's content is as follows:

- Sensitive ant colony optimization (SACO) for medical image edge detection is introduced to improve the analysis of CT and X-ray images.
- Image pre-processing is done.
- The use of several demi-contractive operators is employed to check their behavior for both ACO and SACO.
- Postprocessing, including the use of the DeNoise convolutional neural network (DnCNN), is done.
- A comparison between ACO, SACO and several state-of-art methods to ensure the validity of the sensitive approach on a CT and X-ray image dataset is made.

The next section includes the present work's prerequisites with mathematical support, the edge detecting problem and the sensitive ant colony optimization (SACO) method. The numerical tests and bio-inspired methods results follows in Section 3. The comparison of methods, the operators' behavior and the representation of medical image results are discussed in Section 4. Future work and arguments regarding the benefits of ACO and SACO for medical images conclude the present study.

2. Prerequisites

Math Operators. At first, a short introduction into the mathematical part of the work is presented; this is, mainly based on Rus [19] who introduced the theory of admissible perturbations of an operator. The admissible perturbation operator was also studied in [20].

Demicontractive operators. As already stated in our previous work [18], a *demicontractive operator* (T) is defined by C, a subset of $\mathbb{R}$ (domains and co-domains). For an existing *contraction coefficient* ($k < 1$), each fixed point (p) of the demicontractive operator and all numbers ($x \in C$) the inequality (1) is true.

$$\|Tx - p\|^2 \leq \|x - p\|^2 + k\|x - Tx\|^2. \tag{1}$$

For a nonempty set (X) and an admissible mapping, ($G : X \times X \to X$), the following statements are true: for all $x \in X$ G(x, x) = x and $G(x, y) = x$ implies $y = x$ [19].

The admissible perturbation of the operator f ($f : X \to X$) [19] is the admissible mapping $f_G : X \to X$ ($f_G(x) := G(x, f(x))$).

Krasnoselskij operator. The *Krasnoselskij algorithm* [19], corresponding to an admissible mapping ($G : X \times X \to X$) of an nonlinear operator ($f : X \to X$), is defined as an iterative algorithm $\{x_n\}_{n\in\mathbb{N}}$ with $x_0 \in X$ and $x_{n+1} = G(x_n, f(x_n))$, where $n \geq 0$.

For further details and examples, see [18,20,21].

The χ operator. The χ operator $\chi : \mathbb{R} \times \mathbb{R} \longrightarrow [0,1)$ is defined as:

$$\chi(x,y) = \frac{x^2 \cdot y^2}{(1+x^2)\cdot(1+y^2)}, \tag{2}$$

where $y : \mathbb{R} \to \mathbb{R}$, $y(x) = \frac{2}{3}x \sin\frac{1}{x}$, if $x \neq 0$.

Particular Math Functions. The operators further used as $f(\cdot)$ in the considered methods (see (8)) are as follows:

Sin: $$f(x) = \sin\left(\frac{\pi x}{2\lambda}\right), \text{ if } 0 \leq x \leq \lambda; \tag{3}$$

KH: $$f(x) = (1-\lambda)\cdot x + \lambda \cdot \frac{2}{3} x \sin\frac{1}{x} \text{ if } x \neq 0; \tag{4}$$

Chi: $$f(x) = (1 - \chi(x, y(x)))\cdot x + \chi(x, y(x)) \cdot y(x) \text{ if } x \neq 0; \tag{5}$$

The functions (3)–(5) are zero in all other possible cases. The λ parameter from Equations (3) and (4) adjusts the operators used as test functions in [22]. In [23], the authors used two admissible perturbation operators for computing the heuristic value required within the ACO algorithm.

In the present article, where admissible perturbations of demicontractive mappings are utilized as test functions, and the PSL vector is utilized for each ant, a sensitivity to the artificial pheromone is introduced using a specific coefficient influenced by the image's intensity values for the edge detection problem.

The ants have different roles in edge extraction: some agents are explorers and others are exploiters; these roles are exchanged as the PSL vector updates during processes. The obtained results for CT and X-ray medical images and the comparison among the results using the proposed operators are made in Section 4.

3. Problem and Methods

3.1. Medical Image Edge Detection Problem

The problem to solve is the edge detection problem. The current work improves solutions of particular medical images due to their complex edges based on X-rays and tomographic images.

Image edge detection involves the detection of discontinuities in brightness while processing the image in order to find the boundaries of objects.

3.2. Sensitive Ant Colony Optimization Method

The method used is an improved version of *Ant Colony Optimization (ACO)* [1] called the *Sensitive Ant Colony Optimization (SACO)* [24,25]. The ant colony optimization sensitive approach for medical image edge detection is further presented. There is considered a colony of K ants engaged in a search within the graph space $\mathcal{X}$, with $M_1 \times M_2$ nodes.

SACO as well as ACO use artificial ants to move in a 2D image in order to build the pheromone matrix; each matrix element represents the edge information for every pixel in the image.

In general, ACO and its versions builds a solution with the use of artificial ants; these agents search for the best path in a given space by depositing artificial pheromones [1,23]. These pheromone trails are updated during the search process.

The ACO and SACO general scheme includes an initialization process followed by N construction steps while creating and updating pheromone matrix, and, finally, performing the decision process to determine a beneficial solution.

Ant colony optimization for edge detection

Initialize ACO parameters
Schedule activities
  Construct ant solutions
  Update pheromone
  Edge detection
End scheduled activities

Initialization process: In particular, for image edge detection with ACO and SACO during the initialization process, the entire ant colony (K ants) places ants randomly on the image matrix. Each image pixel is considered to be a node in a graph. Each initial pheromone matrix $\tau_{(0)}$ has a constant τ_{init} value. A constant value L defines the number of moves during the construction process.

For SACO in particular, each PSL vector component is initialized with 1, starting as the original ACO (see Figure 1).

Figure 1. Symbolic illustration of the sensitive ant model showing the ants' probability variation within the unit interval from the ACO probability when $PSL = 1$ to a random walk probability when $PSL = 0$.

Construction phase: at the n-th construction step, a randomly chosen ant will move from node i to j according to the transition probability in (6) for L steps.

$$p_{ij}^{n} = \frac{\left(\tau_{ij}^{(n-1)}\right)^{\alpha}\left(\eta_{ij}\right)^{\beta}}{\sum_{j\in\Omega_i}\left(\tau_{ij}^{(n-1)}\right)^{\alpha}\left(\eta_{ij}\right)^{\beta}}, \qquad \text{if } j \in \Omega_i, \tag{6}$$

where τ_{IJ} is the pheromone value on (i,j); η_{IJ} the heuristic value connecting nodes i and j the same for all n construction steps; α and β are the weighting factors for the pheromone and the heuristic; and Ω_i includes the neighborhood nodes of node i.

The overall eight-connectivity neighborhood for each pixel $I_{i,j}$ within the local configuration at the $I_{i,j}$ pixel, $cI_{i,j}$, for computing the variation value $V_c(I_{i,j})$ defined by (8) is illustrated in [18].

Here, we propose the computation of $\eta_{i,j}$ according to the local statistic of the pixel (i,j) (Equation (7)).

$$\eta_{i,j} = \frac{1}{Z} \cdot V_c(I_{i,j}), \tag{7}$$

where $Z = \sum_{i=1}^{M_1}\sum_{j=1}^{M_2} V_c(I_{i,j})$ is a normalization factor, $I_{i,j}$ is the intensity value of the image pixel (i,j); and the function $V_c(I_{i,j})$ processes the "clique" $cI_{i,j}$ [22].

The $V_c(I_{i,j})$ value at pixel $I_{i,j}$ is influenced by the image's intensity values for $cI_{i,j}$, and its value is [22]:

$$\begin{aligned} V_c(I_{i,j}) = \; & f\big(\left|I_{i-2,j-1} - I_{i+2,j+1}\right| + \left|I_{i-2,j+1} - I_{i+2,j-1}\right| \\ & + \left|I_{i-1,j-2} - I_{i+1,j+2}\right| + \left|I_{i-1,j-1} - I_{i+1,j+1}\right| \\ & + \left|I_{i-1,j} - I_{i+1,j}\right| + \left|I_{i-1,j+1} - I_{i+1,j-1}\right| \\ & + \left|I_{i-1,j+2} - I_{i+1,j-2}\right| + \left|I_{i,j-1} - I_{i,j+1}\right|\big). \end{aligned} \tag{8}$$

In order to validate an edge within the solution, a decision is made for each image pixel by applying a threshold T (see [26]) to the final pheromone matrix $\tau^{(N)}$.

The artificial pheromone matrix values are updated both locally and globally.

Locally update the pheromone matrix τ. The local pheromone matrix update is made after each ant moves within each construction step [22].

$$\text{Local update:} \quad \tau_{ij}^{(n)} = \tau_{ij}^{n-1} \cdot (1-\rho) + \rho \cdot \Delta_{ij}. \tag{9}$$

Notations: ρ is the pheromone evaporation rate, and Δ_{ij} is the artificial pheromone laid on edge (ij).

Globally update the best tour's PSL vector and pheromone matrix τ. The global update occurs after all ants finish all construction steps. Now, the PSL vector recording the pheromone sensitivity level for each ant is also updated according to a specified linear formula based on [24,25]; for this particular problem, the Equation (10) PSL update influenced by the image's intensity values is used.

$$PSL = ((1-\rho) * PSL + \rho * \Delta_{ij} * v(I_{ij})) * \Delta_{ij} + PSL * |1 - \Delta_{ij}|. \tag{10}$$

Furthermore, the best tour is a user defined criterion; it can be the best tour found in the current construction step, or the best tour from the start of the ACO algorithm, or a combination of these two.

For ACO, global update of the pheromone matrix [1] is performed as in Equation (11).

$$\text{Global update ACO:} \quad \tau^{(n)} = (1-\psi) \cdot \tau^{(n-1)} + \psi \cdot \tau^{(0)}, \tag{11}$$

where ψ is the pheromone decay rate.

For *SACO*, the global update is based on its sensitivity feature (Equation (12)).

$$\text{Global update SACO:} \quad \tau^{(n)} = \max_{k=1:K} PSL(k) \cdot \tau^{(n-1)}. \tag{12}$$

The problem solution is obtained after reaching a stopping criteria, such as, for example, a maximal number of iterations.

4. Experiments and Discussions

The numerical experiments were carried out using Matlab on an AMD Rysen 5 2500U, 2GHz. The software is a version of the image edge detection using Ant Colony Optimization version 1.2.0.0. from MATLAB Central File Exchange [27]. The MATLAB implementation [28] of the Canny edge detection algorithm is based on [15].The software makes use of two thresholds in order to detect strong and weak edges; the weak edges are provided in the solution only if they are connected to the strongest ones: "a high threshold for low edge sensitivity and a low threshold for high edge sensitivity", as is specified in the software documentation [28]. In order to convert a gray-scale input image to a binary image, thresholding is used.

Data set. A dataset of medical images, free of copyright, was used for these experiments: *Brain CT* (could be provided by request from the authors), *Hand X-ray* [29], (reduced resolution from 225 × 225 to 128 × 128) and *Head CT* [30]. Several details are included in the Github page (Representation of results available at https://github.com/cristina-ticala/Sensitive_ACO; accessed on October 2021).

Filtering. In order to filter the medical images, the De-Noise convolutional neural network (DnCNN) was used in the present study, as well as in our previous related work [18]. The Image Processing Toolbox and Deep Learning Toolbox from Matlab [31] were used.

Parameters. Most of the parametric numbers are from [22]. In our previous work [18], we tested several parameters; in the present study, we used the best of them.

Image-related parameters: The image dimension influences and gives ACO and SACO a number of artificial ants $K = \lfloor \sqrt{M1 \times M2} \rfloor$, where $\lfloor$ and $\rfloor$ are the left and right rounded values to the nearest integers less than or equal to x; e.g., for a 128×128 image resolution, the number of ants is considered 128.

Iterations related parameters: In [18] just 30,000 iterations for $L = 100$ steps were considered; here, we tested a smaller (1200 iterations for $L = 4$ steps) and a higher number of steps $L = 1000$ (300,000 iterations). An ant makes 300 moves at each step; e.g., for 128 ants (e.g. image resolution: 128×128), 38,400 moves are made during each step. Therefore, for $L = 4$, it is a total of 153,600 moves, 3,840,000 moves for $L = 100$ and a total of 38,400,000 ants' moves for $L = 1000$ steps.

Connectivity-related parameters: The connectivity neighborhood parameter $\Sigma = 8$ is based on the ants' movement range (Equation (6)).

Pheromone trail parameters: the value of each matrix component $\tau_{init} = 0.0001$; the weighting factors of pheromone information $\alpha = 1$ and of heuristic information $\beta = 0.1$ (Equation (6)); the evaporation rate, ρ, is 0.1 (Equation (9)) and the value of the pheromone decay coefficient ψ is 0.001 (Equation (12)).

Other parameters: The adjusting factor λ of the functions (Equations (3)–(5)) is 10. The tolerance parameter ($\varepsilon = 0.1$) is used in the decision process. The stopping criterion is given by the maximal number of steps (L) set by the user.

Comparison: Beside the Canny algorithm, the Roberts, the Sobel and Prewitt edge algorithms were also used for comparison; the last two methods compute the horizontal and the vertical gradient of an image by using two orthogonal filter kernels, and after filtering, they compute the gradient magnitude and apply a threshold in order to find the regions of the image corresponding to the edges. Furthermore, the Roberts algorithm detects image edges at angles of 45 degrees and/ or 135 degrees from horizontal [32].

Table 1. The best number of correctly identified number of pixels, standardized using the overall average and standard deviation for all considered medical images, with every considered operator on all considered algorithms results for sensitive (SACO) and original ACO with DnCNN.

	Head CT		**Brain CT**		**Hand X-ray**	
	ACO	**SACO**	**ACO**	**SACO**	**ACO**	**SACO**
			1200 iterations			
Sin	0.2694	0.4137	−0.1265	0.0111	0.0346	0.0547
KH	−0.3379	−0.2406	−0.1366	0.0648	−0.6616	−0.5778
Chi	−0.3261	−0.3127	−0.1550	−0.1533	−0.7975	−0.6549
			30,000 iterations			
Sin	0.4875	0.4154	−0.0862	0.0815	0.0312	0.0547
KH	−0.2842	−0.2355	−0.0342	0.0614	−0.6214	−0.5627
Chi	−0.3798	−0.3127	−0.2372	−0.1500	−0.7036	−0.6549
			300,000 iterations			
Sin	0.4322	0.4154	−0.0980	0.0765	−0.0124	0.0547
KH	−0.2691	−0.2355	−0.1080	0.0614	−0.6080	−0.5627
Chi	−0.3882	−0.3127	−0.2221	−0.1500	−0.7841	−0.6549

Table 2. The best number of the correctly identified number of pixels, standardized using the overall average and standard deviation for all considered medical images, with every considered operator on all considered algorithms results for Canny edge detection [15], as well as the Prewitt, Sobel, and Roberts methods [32].

	Head CT	**Brain CT**	**X-ray**
Canny	−1.4166	−1.4803	−1.2857
Prewitt	−2.4567	−2.6865	−2.7721
Sobel	−2.4751	−2.5926	−2.7486
Roberts	−3.0606	−2.8878	−2.9130

Running time. The average running time was around 4500 seconds for both ACO and SACO with the presented parameters on the utilized computer.

Table 1 shows the best, maximal results of the number of correctly identified pixels standardized using the overall average, $Avg = 2107.030303$, and standard deviation, $StdDev = 563.50$, for all considered medical images, and operators on the sensitive ant colony method (SACO) and ACO denoised with DnCNN. Table 2 shows the Canny [15], Prewitt, Sobel and Roberts methods results and Table 3 illustrates the original ACO and SACO results before post-processing with DnCNN.

Table 3. The best number of correctly identified number of pixels, standardized using the overall average and standard deviation for all considered medical images, with every considered operator on all considered algorithms; results for sensitive (SACO) and original ACO methods.

	Head CT		**Brain CT**		**Hand X-ray**	
	ACO	**SACO**	**ACO**	**SACO**	**ACO**	**SACO**
1200 iterations						
Sin	1.5863	1.5729	0.7123	0.9187	1.0512	0.9153
KH	0.6871	0.8029	0.6905	0.9371	0.1637	0.1637
Chi	0.8281	0.6335	0.5714	0.6184	−0.0476	0.0799
30,000 iterations						
Sin	1.5981	1.5746	0.8801	0.9690	0.9187	0.9153
KH	0.8096	0.8046	0.8499	0.9354	0.1553	0.1755
Chi	0.5949	0.6351	0.5596	0.6200	0.0262	0.0799
300,000 iterations						
Sin	1.5528	1.5746	0.7777	0.9656	0.9338	0.9153
KH	0.7928	0.8046	0.7777	0.9371	0.1855	0.1755
Chi	0.6569	0.6335	0.5781	0.6200	−0.0443	0.0799

The best solutions obtained for the considered medical images (Head CT, Brain CT and Hand X-ray) while comparing ACO and SACO for 300,000 iterations and the considered demicontractive operators are included in Figure 2; in the last image, the original medical images are overlapped with the best solutions.

Analysis. The values are already standardized based on the denoised ACO and SACO, Canny, Prewitt, Sobel, and Roberts results; therefore, the difference between SACO and ACO is significant from an analytic perspective.

- *An operator comparison analysis* based on Figure 3 uses the difference of SACO vs. ACO values; for the Sin-operator, the difference has a majority of negative values, with ACO obtaining better values than SACO for the considered operators (44.45%); for the other two operators, χ-operator (Chi) and KH-operator, 77.78% shows SACO performing better than ACO on the 9 considered cases of medical images;
- *Medical image analysis.* For each medical image, including head CTs, brain CTs and hand X-rays, Figure 3 identifies operators' behavior on the difference between SACO and AC0. The lowest SACO performance, 44.44%, was obtained for the head CT medical images; its highest performance was 100% for the brain CT images, while for the hand X-rays, a 55.56% performance value was obtained. The percentage is based on the number of considered medical images.

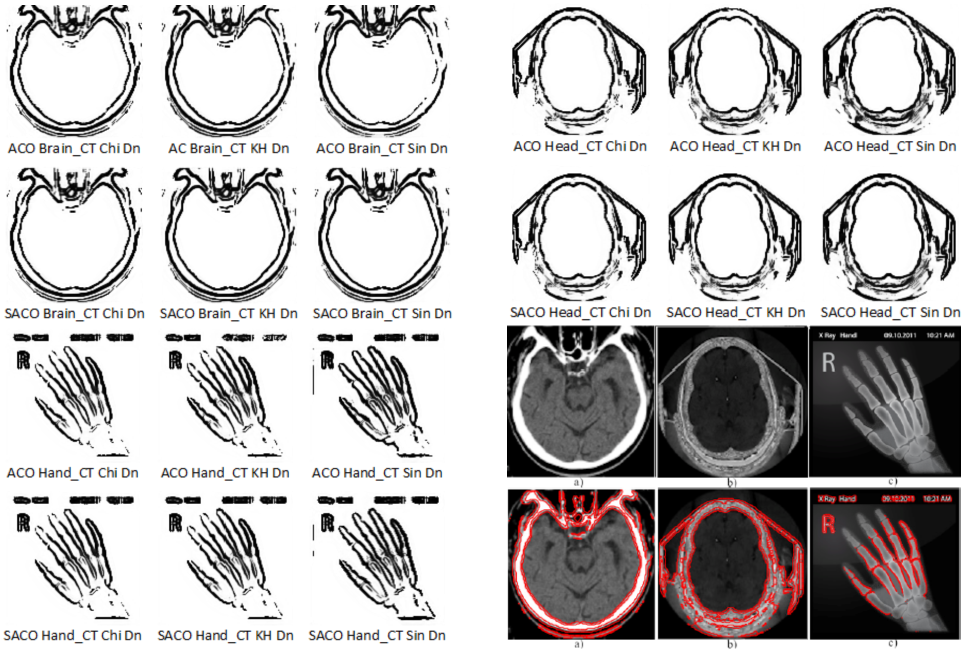

Figure 2. Successive illustrations of the best solutions obtained after 300,000 iterations with *Ant colony optimization (ACO)* and *Sensitive ACO (SACO)* post-processed with the *Denoise Convolutional Neural Network (DnCNN)* and the overlapped best solutions' edges over the original medical images for (**a**) Brain CT; (**b**) Head CT and (**c**) Hand X-ray.

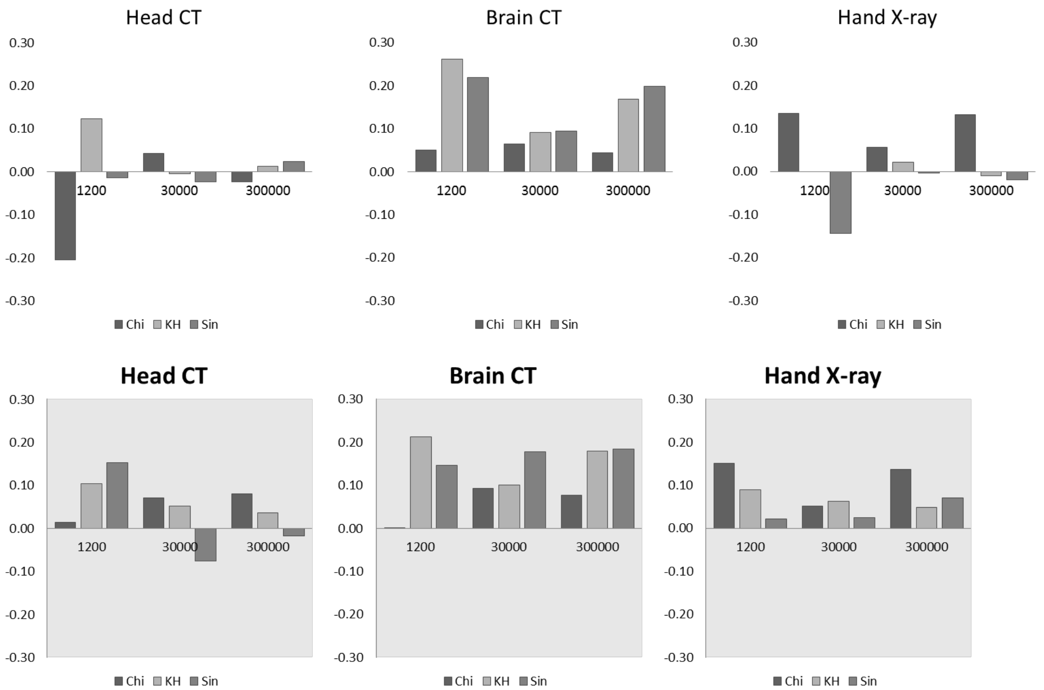

Figure 3. Head CT, Brain CT and Hand X-ray results based on the difference between SACO and ACO standardized values, before (up) and after post-processing with the DeNoise convolutional neural network (DnCNN) (down).

Stability & quality of the solutions. The quality of the partial solution is influenced by the amount of modified pheromone of the ants' trail.

The stability of the global solution is influenced by used parameters. The included PSL parameter hopefully influenced the global solution for the better.

The global solution is found after the entire ant colony, based on the existing pheromone information, is guided to more promising regions in the search space.

The pheromone sensitivity factor balances the exploring and exploiting activities; its value is a number from $[0, 1]$. An ant ignores information when $PSL = 0$ and has the maximum pheromone sensitivity when $PSL = 1$.

- *An exploring search* is made by independent ants with a low PSL value.
- *An exploiting search* is made by sensitive ants to pheromone traces, the intensively exploitative ants with a high PSL value.

In time, the process modifies ants' pheromone sensitivity (PSL). In the current work, the PSL is globally modified (increased or decreased) by the search space topology [17].

SACO advantages. By adding the PSL vector, the present algorithm offers the stability of its solutions; for the considered examples, after around 300 iterations, SACO generated edges which almost overlapped over the original images. As a plus, the image edge results are much more compact and close to the original when compared with the ACO results.

SACO disadvantages. As the number of parameters increases, the user should properly configure their values. This could take more time and resources, but the improved results are worth the effort.

Figure 4 shows the improvements of SACO-DnCNN compared to the Canny, Prewitt, Sobel and Roberts edge detection techniques [32]. The best SACO-DnCNN results, using χ, outperform the Canny Edge detector results by 37.76%; the Prewitt, Sobel and Roberts [32] methods were significantly outperformed by over 159%, 157% and 224%.

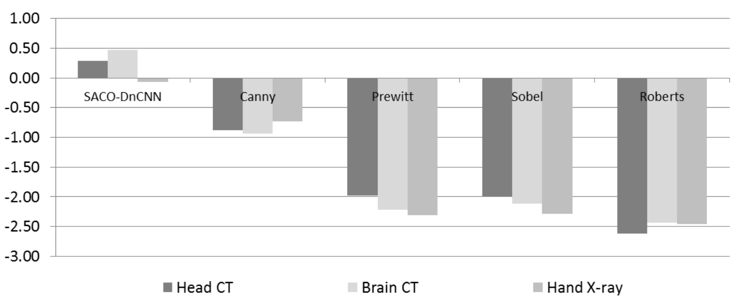

Figure 4. Comparison of the best SACO-DnCNN, Canny, Prewitt, Sobel, and Roberts methods on the Head CT, Brain CT and Hand X-ray medical images.

Future work will use images with higher resolutions, and hopefully the impact of sensitivity will improve the problem solutions.

Future work will also include implementing specific ACO and SACO features to solve publicly available medical datasets, including COVID- and SARS-Cov-2-related data sets. Furthermore, sensitivity for different artificial intelligence models could be involved within different domains, e.g., data mining [33] and similar.

Other improvements could utilize fuzzy techniques and multiple ant colonies for ACO, as in [34], which could be used to enhance the solutions for image edge detection.

Further work could make use of image segmentation with edge detection in order to obtain a more thorough edge [35]. As prerequisites for the development of knowledge-based applications, ontologies for the segmentation of radiological images [36] were proposed by the authors.

Other metaheuristics, mostly bio-inspired ones [37], could be further enhanced with sensitivity features in order to improve the results of complex problems. Human-in-the-loop [38] could also enhance the problem results.

5. Conclusions

Medical image edge detection is nowadays a must in the context of pandemics and other illness and injuries. As classical algorithms have less performance within image edge detection, metaheuristics are used for feasible solutions. The current paper shows the efficiency of bio-inspired algorithms, in particular of the ant-based technique, with an emphasis on the sensitive version of *Ant Colony Optimization (ACO)*.

Sensitivity plays a crucial role in the exploration and exploitation of ants' solutions within the environment; the sensitivity level starts with the maximum level of sensitivity, one, per the ACO level of sensitivity, and during the processes, the ant's level of sensitivity changes. they become less or more sensitive to the environment based on the PSL probability, which is influenced by ants behavior and image intensity.

Nevertheless, the demicontractive operators shows their utility in edge detection problems; an analysis of the results with the presented operators shows how the results vary based on the operators' features.

The edges obtained with each considered operator were overlapped over the original images. The majority of edges were superposed, following the CT and X-ray original bone lines.

Author Contributions: Conceptualization, investigation C.T. and C.-M.P.; methodology formal analysis C.T. and O.M., software, C.T.; validation C.T. and O.M.; writing—original draft preparation C.T. and C.-M.P. and O.M.; writing—review and editing C.T. and C.-M.P. All authors have read and agreed to the published version of the manuscript.

Funding: This research received no external funding.

Conflicts of Interest: The authors declare no conflict of interest.

Abbreviations

The following abbreviations are used in this manuscript:

ACO	Ant Colony Optimization
SACO	Sensitive Ant Colony Optimization
DnCNN	Denoise Convolutional Neural Network

References

1. Dorigo, M.; Stützle, T. *Ant Colony Optimization*; MIT Press: Cambridge, MA, USA, 2004.
2. Marginean, A.N.; Muntean, D.D.; Muntean, G.A.; Priscu, A.; Groza, A.; Slavescu, R.R.; Pintea, C.M. Reliable learning with PDE-based CNNs and dense nets for detecting COVID-19, pneumonia, and tuberculosis from chest X-ray images. *Mathematics* **2021**, *9*, 434. [CrossRef]
3. Chattopadhyay, S.; Dey, A.; Singh, P.K.; Geem, Z.W.; Sarkar, R. Covid-19 Detection by Optimizing Deep Residual Features with Improved Clustering-Based Golden Ratio Optimizer. *Diagnostics* **2021**, *11*, 315. [CrossRef] [PubMed]
4. Castiglione, A.; Vijayakumar, P.; Nappi, M.; Sadiq, S.; Umer, M. COVID-19: Automatic Detection of the Novel Coronavirus Disease From CT Images Using an Optimized Convolutional Neural Network. *IEEE Trans. Ind. Inform.* **2021**, *17*, 6480–6488. [CrossRef]
5. Voβ, S.; Martello, S.I.H.; Roucairol, C. (Eds.) *Meta-Heuristics: Advances and Trends in Local Search Paradigms for Optimization*; Publisher: Springer Science & Business Media: Berlin/Heidelberg, Germany, 2012.
6. Voβ, S. Meta-heuristics: The state of the art. In *Workshop on Local Search for Planning and Scheduling*; Springer: Berlin/Heidelberg, Germany, 2000; pp. 1–23.
7. Liantoni, F.; Rozi, N.F.; Indriyani, T.; Rahmawati, W.M.; Hapsari, R.K. Gradient based ant spread modification on ant colony optimization method for retinal blood vessel edge detection. *Iop Conf. Ser. Mater. Sci. Eng.* **2021**, *1010*, 012021. [CrossRef]
8. Li, J.; An, X. Efficient Filtering for Edge Extraction under Perspective Effect. *Appl. Sci.* **2021**, *11*, 8558. [CrossRef]
9. Crisan, G.C.; Nechita, E.; Palade, V. Ant-based system analysis on the traveling salesman problem under real-world settings. In *Combinations of Intelligent Methods and Applications*; Springer: Cham, Switzerland, 2016; pp. 39–59.
10. Paprocka, I.; Krenczyk, D.; Burduk, A. The Method of Production Scheduling with Uncertainties Using the Ants Colony Optimisation. *Appl. Sci.* **2021**, *11*, 171. [CrossRef]
11. Matei, O.; Rudolf, E.; Pintea, C.M. Selective Survey: Most Efficient Models and Solvers for Integrative Multimodal Transport. *Informatica* **2021**, *32*, 371–396. [CrossRef]
12. Vescan, A.; Pintea, C.M.; Pop, P.C. Test Case Prioritization-ANT Algorithm with Faults Severity. *Logic J. IGPL* **2020**, *29*, jzaa061. [CrossRef]
13. Pintea, C.-M.; Pop, P.C. Sensor networks security based on sensitive robots agents. A conceptual model. *Adv. Intell. Syst. Comput.* **2013** *189*, 47–56. [CrossRef]

14. Pintea, C.-M.; Pop, P.C. Sensitive Ants for Denial Jamming Attack on Wireless Sensor Network. *Adv. Intell. Soft Comput.* **2014**, *239*, 409–418. [CrossRef]
15. Canny, J. A Computational Approach to Edge Detection. *IEEE Trans. Pattern Anal. Mach. Intell.* **1986**, *PAMI-8*, 679–698. [CrossRef]
16. Zhang, Z.; Liu, Y.; Liu, T.; Li, Y.; Ye, W. Edge Detection Algorithm of a Symmetric Difference Kernel SAR. Image Based on the GAN Network Model. *Symmetry* **2019**, *11*, 557. [CrossRef]
17. Pintea, C.-M.; Ticala, C. Medical image processing: A brief survey and a new theoretical hybrid ACO model. In *Combinations of Intelligent Methods and Applications. Smart Innovation, Systems and Technologies*; Springer: Cham, Switzerland, 2016; Volume 46, pp. 117–134. [CrossRef]
18. Ticala, C.; Zelina, I.; Pintea, C.-M. Admissible Perturbation of Demicontractive Operators within Ant Algorithms for Medical Images Edge Detection. *Mathematics* **2020**, *8*, 1040. [CrossRef]
19. Rus, I.A. An abstract point of view on iterative approximation of fixed points. *Fixed Point Theory* **2012**, *33*, 179–192.
20. Berinde, V.; Ticala, C. Enhancing Ant-Based Algorithms for Medical Image Edge Detection by Admissible Perturbations of Demicontractive Mappings. *Symmetry* **2021**, *13*, 885. [CrossRef]
21. Ticala, C. A weak convergence theorem for a Krasnoselskij type fixed point iterative method in Hilbert spaces using an admissible perturbation. *Sci. Stud. Res.* **2015**, *25*, 243–252.
22. Tian, J.; Yu, W.; Xie, S. An ant colony optimization algorithm for image edge detection. In Proceedings of the 2008 IEEE Congress on Evolutionary Computation (IEEE World Congress on Computational Intelligence), Hong Kong, China, 1–6 June 2008; pp. 751–756.
23. Ticala, C.; Zelina, I. New ant colony optimization algorithm in medical images edge detection. *Creat. Math. Inf.* **2020**, *29*, 101–108. [CrossRef]
24. Pintea, C.M.; Chira, C.; Dumitrescu, D.; Pop, P.C. A sensitive metaheuristic for solving a large optimization problem. *Lect. Notes Comput. Sci.* **2008**, *4910*, 551–559. [CrossRef]
25. Chira, C.; Dumitrescu, D.; Pintea, C.M. Learning sensitive stigmergic agents for solving complex problems. *Comput. Inform.* **2010**, *29*, 337–356.
26. Otsu, N. A threshold selection method from gray-level histograms. *IEEE Trans. Syst. Man Cybern.* **1979**, *9*, 62–66. [CrossRef]
27. Kanchi-Tian, J. *Image Edge Detection Using Ant Colony Optimization Version 1.2.0.0*; MATLAB Central File Exchange; University of Science & Technology: Wuhan, China, 2011.
28. Edge Function. MATLAB Central File Exchange. Available online: https://www.mathworks.com/help/images/ref/edge.html (accessed on 5 August 2021).
29. X-ray Hand. Vista Medical Pack. License: Free for Non Commercial Use. p. 236487. Available online: https://www.iconspedia.com/ (accessed on 5 August 2021).
30. Head CT. Online Medical Free Image. Available online: http://www.libpng.org/pub/png/pngvrml/ct2.9-128x128.png (accessed on 5 August 2021).
31. Denoise Image Using Deep Neural Network. MATLAB Central File Exchange. Available online: https://www.mathworks.com/help/images/ref/denoiseimage.html (accessed on 5 August 2021).
32. Kumar, S.; Upadhyay, A.K.; Dubey, P.; Varshney, S. Comparative analysis for Edge Detection Techniques. In Proceedings of the 2021 International Conference on Computing, Communication, and Intelligent Systems (ICCCIS), Greater Noida, India, 19–20 February 2021; pp. 675–681.
33. Avram, A.; Matei, O.; Pintea, C.; Anton, C. Innovative Platform for Designing Hybrid Collaborative & Context-Aware Data Mining Scenarios. *Mathematics* **2020**, *8*, 684. [CrossRef]
34. Pintea, C.M.; Matei, O.; Ramadan, R.A.; Pavone, M.; Niazi, M.; Azar, A.T. A Fuzzy Approach of Sensitivity for Multiple Colonies on Ant Colony Optimization. *Soft Comput. Appl.* **2016**, *634*, 87–95. [CrossRef]
35. Ahn, E.; Kim, J.; Bi, L.; Kumar, A.; Li, C.; Fulham, M.; Feng, D.D. Saliency-Based Lesion Segmentation via Background Detection in Dermoscopic Images. *IEEE J. Biomed. Health Inform.* **2017**, *21*, 1685–1693. [CrossRef] [PubMed]
36. Matei, O. Defining an ontology for the radiograph images segmentation. In Proceedings of the 9th International Conference on Development and Application Systems, Suceava, Romania, 22–24 May 2008; pp. 266–271.
37. Abd, E.M.; Ewees, A.A.; Ibrahim, R.A.; Lu, S. Opposition-based moth-flame optimization improved by differential evolution for feature selection. *Math. Comput. Simul.* **2020**, *168*, 48–75.
38. Holzinger, A.; Plass, M.; Kickmeier-Rust, M.; Holzinger, K.; Crişan, G.C.; Pintea, C.M.; Palade, V. Interactive machine learning: Experimental evidence for the human in the algorithmic loop: A case study on Ant Colony Optimization. *Appl. Intell.* **2019**, *49*, 2401–2414. [CrossRef]